

Effect of geometric sharpness on translucent material perception

Bei Xiao

Department of Computer Science, American University,
Washington, DC, USA



Shuang Zhao

Department of Computer Science, University of
California, Irvine, Irvine, CA, USA



Ioannis Gkioulekas

Robotics Institute, Carnegie Mellon University,
Pittsburgh, PA, USA



Wenyan Bi

Department of Computer Science, American University,
Washington, DC, USA



Kavita Bala

Computer Science, Cornell University, Ithaca, NY, USA



When judging the optical properties of a translucent object, humans often look at sharp geometric features such as edges and thin parts. An analysis of the physics of light transport shows that these sharp geometries are necessary for scientific imaging systems to be able to accurately measure the underlying material optical properties. In this article, we examine whether human perception of translucency is likewise affected by the presence of sharp geometry, by confounding our perceptual inferences about an object's optical properties. We use physically accurate simulations to create visual stimuli of translucent materials with varying shapes and optical properties under different illuminations. We then use these stimuli in psychophysical experiments, where human observers are asked to match an image of a target object by adjusting the material parameters of a match object with different geometric sharpness, lighting, and three-dimensional geometry. We find that the level of geometric sharpness significantly affects perceived translucency by observers. These findings generalize across a few illumination conditions and object shapes. Our results suggest that the *perceived* translucency of an object depends on both the underlying material's optical parameters and the three-dimensional shape of the object. We also find that models based on image contrast cannot fully predict the perceptual results.

Introduction

Many real-world materials are translucent, and humans interact with such materials often in their

Citation: Xiao, B., Zhao, S., Gkioulekas, I., Bi, W., & Bala, K. (2020). Effect of geometric sharpness on translucent material perception. *Journal of Vision*, 20(7):10, 1–17, <https://doi.org/10.1167/jov.20.7.10>.

<https://doi.org/10.1167/jov.20.7.10>

Received July 23, 2018; published July 14, 2020

ISSN 1534-7362 Copyright 2020 The Authors

every day lives. Examples include human skin, most foods, minerals, wooden objects, and chemical products (e.g., soap and wax). Compared with opaque materials, translucent ones have a characteristic appearance that results from light penetrating their surfaces, scattering internally, and eventually reemerging from different surface locations. This kind of light-material interaction is known as *subsurface scattering* (Ishimaru, 1991). The ubiquity and importance of translucent materials has long motivated research toward modeling and understanding their appearance. In recent years, there has been significant progress in developing rendering algorithms and representations that, by modeling the underlying physics, can create realistic reproductions of translucency (Jensen et al., 2001; Donner & Jensen, 2008; Gkioulekas et al., 2013). As with physics, there have likewise been previous efforts trying to decipher the other major aspect of translucent appearance, namely, its *perception* by the human visual system (Fleming & Bühlhoff, 2005; Motoyoshi, 2010; Anderson, 2011; Nagai et al., 2013; Gkioulekas et al., 2013; Xiao et al., 2014; Chowdhury et al., 2017; Marlow et al., 2017; Sawayama et al., 2019). Despite these efforts, our understanding of translucency perception remains limited.

The study of the perception of translucency is confounded by the fact that there exists a tight coupling between how humans perceive the illumination, shape, and material properties of translucent objects (Xiao et al., 2014; Marlow et al., 2017). Recently, Chowdhury et al. (Chowdhury et al., 2017) showed that the perception of the three-dimensional (3D) shape of a translucent object is different from that of an opaque one. They



created stimuli by manipulating the spatial frequency of relief surfaces for both translucent and opaque objects. Using these stimuli, they found that observers judged translucent objects to have fewer bumps than opaque objects with the same 3D shape. Additionally, they observed that the perceived local curvature was underestimated for translucent objects relative to opaque objects.

Motivated by these intriguing findings, in this article we continue the investigation of the interplay between the perception of 3D shape and material for translucent objects. We focus on a specific type of geometric feature, namely, thin geometric structures such as edges and depth discontinuities. We use the term *geometric sharpness* to refer broadly to the presence of such features. Our focus on geometric sharpness is justified from previous studies in both physics (Zhao et al., 2014; Gkioulekas et al. 2015) and perception (Fleming & Bühlhoff, 2005; Gkioulekas et al., 2013), indicating that the presence of thin geometric features is critical for discriminating between translucent materials. In particular, we investigate the following questions:

- How does geometric sharpness affect the perception of translucent material properties?
- Can we manipulate geometric sharpness to make an object appear more or less translucent?

To answer these questions, we first review related previous work in Section 2. Then, we start our investigations by synthesizing a large number of image stimuli, with greatly varying 3D shapes, illumination, and optical properties, detailed in Section 3. We use these stimuli to conduct psychophysical studies, the results of which are statistically analyzed in Section 4. Finally, in Section 5, we discuss implications of our experimental results. Specifically, our findings indicate that 3D geometric sharpness affects translucent material perception in such a way that blurring geometric details cause objects to appear more translucent than objects with sharp geometry. The effect can be generalized to two different lighting conditions and both positive and negative relief conditions. However, the effect is stronger for optically dense (less translucent) materials. In addition, we find models based on global image contrasts cannot fully predict observer's results because the relationship between image contrasts with the effect of geometric blur is different for objects with low relief from those for objects with high relief.

Previous work

Illumination, material properties, and 3D shape all contribute to the retinal two-dimensional (2D) image that humans perceive. The human visual system subsequently uses these images, among other things,

to infer material properties of the objects contained in them. In this process, the visual system takes into account the effects of ancillary shape and illumination properties (Barron & Malik, 2015).

Previous studies on the perception of opaque objects have demonstrated that the shape of an object can affect its perceived material properties (Todd & Mingolla, 1983; Vangorp et al., 2007; Ho et al., 2008; Wijntjes & Pont, 2010; Kim et al., 2012; Marlow & Anderson, 2013, 2015). By varying the surface geometry, it is possible to influence how glossy an object is perceived by human observers to a significant extent. For example, Kim et al. (2016) show that perceived 3D shape plays a decisive role in perception of surface glow. Specifically, by manipulating cues to 3D shape while holding other image features constant, the perception of glow can be toggled on and off.

Conversely, the perception of 3D shape is affected by a surface's optical (i.e., reflectance) properties. For example, it has been shown that the same surface can be perceived to have different 3D geometry when its reflectance becomes more or less specular (Doerschner et al., 2013; Adams & Elder, 2014; Sawayama & Nishida, 2018). This coupling between the perception of 3D shape and surface reflectance properties has also been demonstrated in objects with nonspecular reflectance (Todd et al., 2014). To mention one example, human observers perceive velvet materials as flatter than matte-painted materials of the same shape (Wijntjes et al., 2012). Illumination also enters into this interplay; previous findings show that changes in the lighting of an object can strongly affect its perceived shape (Norman et al., 2004; Mooney et al., 2019) and reflectance (Olkkonen & Brainard, 2011; Marlow et al., 2012).

Similar to human perception of opaque objects, it has been shown that humans also use a variety of image cues to detect subtle differences between translucent objects, as well as to make qualitative inferences about their optical parameters (Fleming et al., 2004; Fleming & Bühlhoff, 2005; Motoyoshi, 2010; Anderson, 2011; Nagai et al., 2013; Gkioulekas et al., 2013). These findings suggest that the perception of translucency is influenced by surface reflectance (gloss versus matte) (Motoyoshi, 2010), illumination conditions (smooth versus harsh) (Xiao et al., 2014), as well as surface geometry (Chowdhury et al., 2017; Marlow et al., 2017). Additionally, it has been suggested that the coupling between the perception of shape and material properties is more complicated for translucent objects than for opaque ones (Anderson, 2011). From the perspective of physics, it has been shown that estimating 3D shape from translucent objects is challenging (Koenderink & Doorn, 2001; Inoshita et al., 2012) and a recent study found that recovered surface normals of shallow relief objects are smoother than opaque objects with the same 3D shape, suggesting volumetric scattering has a blurring effect on photometric normals (Moore &



Figure 1. **(A)** Photograph of a translucent soap bar with surface relief. Previous work indicates that the sharp edges of translucent objects provide rich physical information about their material properties. Our findings indicate that sharp edges are also an important cue for how these material properties are perceived by humans. **(B)** Inspired by this photograph, we render synthetic translucent images with a similar relief geometry, and use images similar to these shown here as stimuli for psychophysical experiments.

Peers, 2013). This finding partially inspired our work to study whether a similar interaction between 3D shape and scattering parameters also exists in perception.

In recent work, Chowdhury et al. (2017) used rendered stimuli that were either opaque or translucent to study the effects of translucent material properties on the perception of 3D shape. In this paper, we study how 3D shape affects the perception of translucency by systematically varying the geometric sharpness and optical density of relief objects. Thus, instead of being opaque or translucent, our stimuli vary in the degree of translucency. Our focus on sharp geometric features is motivated by prior research on the physics of light scattering, which shows that imaging systems can only accurately measure scattering parameters in the presence of such features (Zhao et al., 2014); and that intensity profiles across geometric edges of translucent objects provide rich information about the object's scattering material (Gkioulekas et al., 2015). Specifically, we design a matching experiment to measure the correlation between geometric sharpness and perceived material translucency. By analyzing the data collected through this experiment, we demonstrate that geometric sharpness indeed affects the perception of translucency for objects with lower reliefs. Specifically, smoother geometry usually leads to higher levels of perceived translucency. Stated differently, when shown two objects with identical optical properties, humans tend to perceive the one with smoother geometric structures as more translucent.

General methods

Stimuli

We generate our visual stimuli using 3D models representing a cube with the characters “target” or “match” raised above the top surface. In our

experiments, we focus on the effect of the geometry of the relief (instead of the cube edges and corners) and only show the top surface. Figure 7 shows examples of the resulting rendered images.

The stimuli are rendered using physically accurate simulation of subsurface scattering, implemented by the Mitsuba renderer (Jakob, 2013). In the following, we provide details about the geometric, illumination, and material models we use for stimuli generation.

Geometry. Figure 3 illustrates the 3D geometry of our rendered objects. In our asymmetric matching experiment, we render different letters for the surface relief for match and target. Besides using different letters, the base (top) surfaces are also slightly different. Here, we use “target” stimuli as examples to illustrate the image examples. The object is modeled as a cube that sits on a flat surface (see Figure 4). We use two-dimensional height fields, applied at the top surface of the cube (size 128 mm × 96 mm × 30 mm), to control the shape of our relief models. The height fields were represented as $z(x,y)$, and by applying low-pass (e.g., Gaussian) filtering to the height field, we can easily manipulate the object's geometric sharpness. The relief heights range from 0.5 mm to 2.5 mm. The kernel standard deviation is ranged from 0.08 mm to 0.56 mm. We use two types of relief as our stimuli in Experiment 1 and Experiment 2. The positive relief has the pattern raised above the top ground surface and the negative relief has the pattern sunken into the ground surface (see Figures 6 and 10 for examples).

Material. We used the radiative transfer framework (Chandrasekhar, 1960) to describe the scattering of light inside translucent objects. Radiative transfer is widely used in applied physics, biomedicine, remote sensing, and computer graphics. Under this framework, the optical properties of a homogeneous translucent material are described using three parameters (see Figure 2):

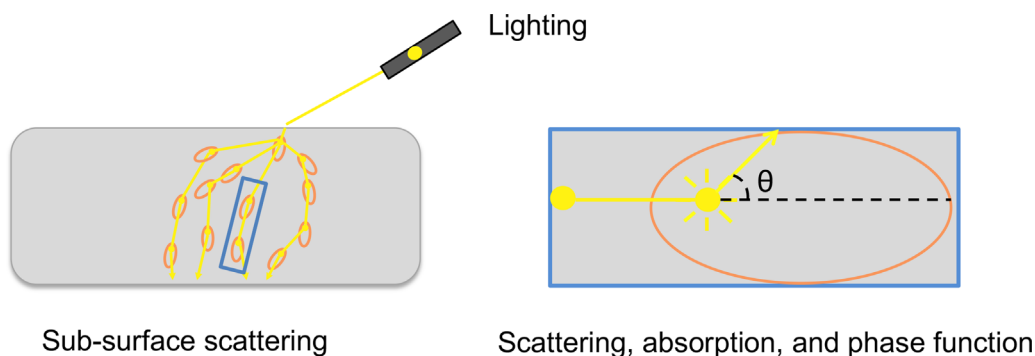


Figure 2. Illustration of the physics of subsurface scattering using the radiative transfer framework. (Left): Translucent appearance is caused by light scattering inside the volume of an object, which can be described by the radiative transfer framework (Chandrasekhar, 1960). (Right): A closer look of subsurface scattering. Between scattering events, light travels for distances determined by the object's extinction coefficient. At each scattering event, light is either absorbed or scattered toward different directions, depending on the object's volumetric albedo. Finally, when light is scattered, the phase function describes the angular distribution of each new direction of travel.

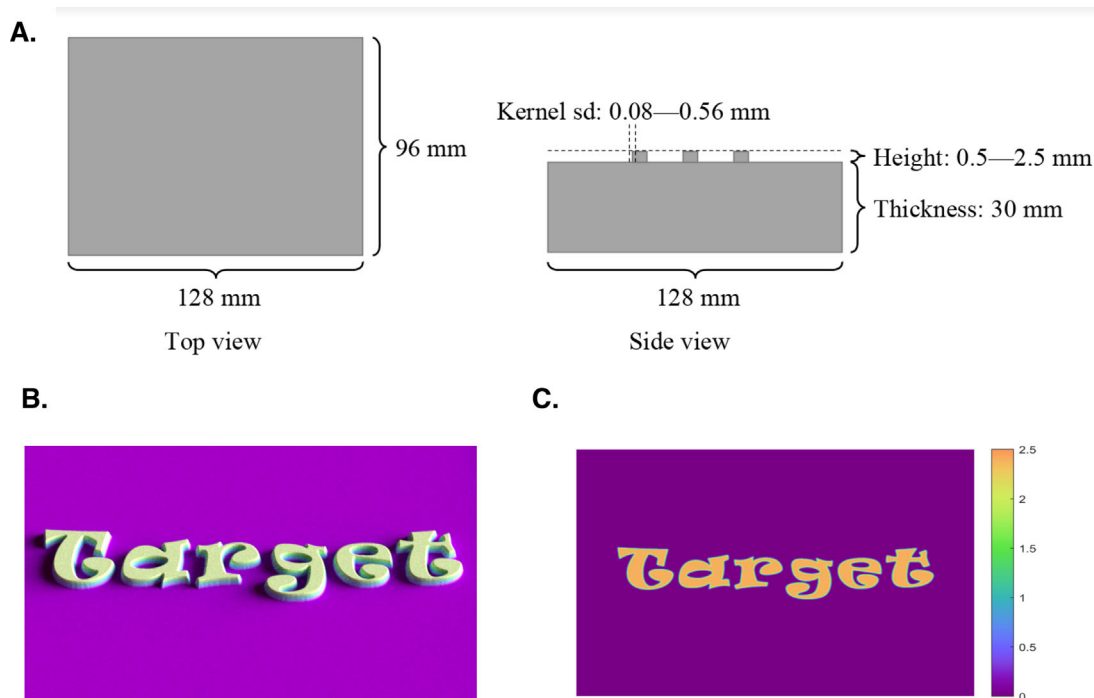


Figure 3. Illustration of the 3D geometry of the rendered objects. (A) Dimensions of the object. (B). 3D model of TARGET object. (C). Height maps of the surface relief. Different colors represent different height (z axis) at each pixel locations.

- *Optical density* is a measure of physical translucency. Also known as the extinction or total attenuation coefficient, it specifies how frequently light scatters within a material. An optical density of $X \text{ mm}^{-1}$ means light on average travels (in straight lines) for $1/X$ mm before being scattered by the medium. Thus, $1/X$ is usually termed as the “mean free path.” A higher density, or a lower mean free path, means more frequent scattering of

light. Optically thin materials (i.e., those with low optical densities) are semi transparent. Optically thick materials, on the other hand, can appear mostly opaque, because as light cannot travel very far inside the material owing to very strong attenuation.

- *Volumetric albedo* determines how much light is absorbed and how much light is scattered to other directions, every time a scattering event takes place.

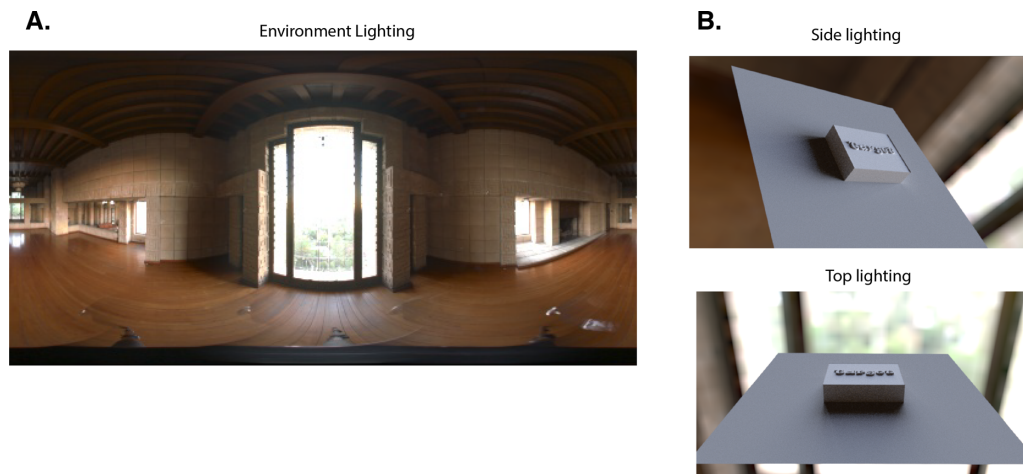


Figure 4. **(A)** The “Ennis” environment map used to generate our stimuli. **(B)** Example renderings of the stimuli object under two lighting conditions. In the “side-lighting” condition, the tall floor window is to the right of the object. But there are also light sources (smaller windows) on the left. In the “top lighting” condition, the light is from above the line of sight and the same tall floor window that provides most direct lighting is behind the object. The viewing direction is toward the floor (of the Ennis room), that is, as if the object is placed on the ground. The camera views of the example renderings are for illustration purpose ONLY and are slightly DIFFERENT from what we used in the paper.

- The *phase function* determines how scattered light is distributed to different directions when scattering events take place.

Lighting. To provide natural illumination, we used environmental lighting for our renderings. Specifically, we used the publicly available “Ennis” lighting environment (see Figure 4) that captures the illumination of the dining room of the Ennis-Brown house in Los Angeles, California (Debevec, 1998). Because this lighting condition is highly directional owing to the bright glass door, we rotated it to create both top lighting and side lighting. The right panels in Figure 4 illustrated the two lighting conditions we used in the experiments with two example renderings. In the side lighting condition, the tall glass door is at the right side of the object while in the top-lighting condition, the tall glass window is behind the object. Because the viewer would look at the object mostly from above, we call this lighting condition top lighting. One can tell the lighting direction by looking at the cast shadows. Our choice of environmental lighting is determined by the observation that materials rendered under natural lighting seem to be more realistic than materials rendered under directional lighting.

To ensure that our matching experiments are asymmetric, we used different extruding characters (geometry) and lighting geometry to render the target and match objects. The lighting directions for both side and top lighting slightly differ from the target and match images (see Figure 5). Specifically, we rotated the environmental map slightly (15°) in the scene depending on whether it is target or match to avoid exactly identical illumination conditions.

Sampling of model parameters

We vary the geometric, material, and lighting properties of the stimuli (see example images in Figure 6).

For geometry, we use reliefs with five heights (0.5, 1.0, 1.5, 2.0, and 2.5 mm), where smaller values indicate lower reliefs. For each height, we apply Gaussian blurring to the underlying height fields using four kernel standard deviations (0.08, 0.2, 0.4, and 0.56 mm). Larger blurring kernels result in stimuli with lower geometric sharpness. The thickness of the rendered object is 30 mm.

For material scattering parameters, we use 15 optical density values sampled logarithmically between 0.7 and 3 (mm^{-1}). We fix volumetric albedo to 0.9 and the phase function to be uniform.

Finally, we render the objects using both side and top environmental lighting. In total, our stimuli dataset consists of 4 (densities) \times 5 (heights) \times 4 (blurs) \times 2 (lightings) = 160 target images. For each target image, we also render 15 (densities) \times 1 (height) \times 1 (blur) \times 1 (lighting) = 15 match images for a different but fixed blur level (with kernel size 0.24 mm). In total, we render 2400 images. The rendering, lighting, and experimental procedure for Experiment 2 (negative relief) is the same as detailed, except for the geometry of the stimuli.

Procedure

We use the asymmetric matching method to obtain psychophysical measures of the perceived translucency (Brainard & Wandell, 1992). Previously,

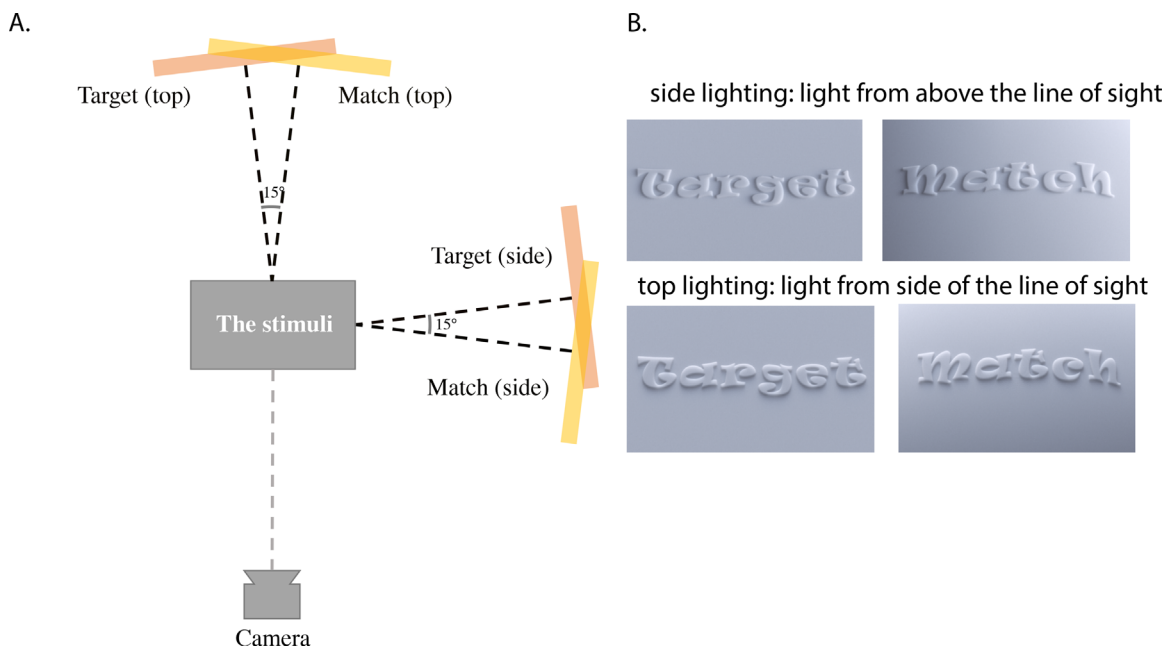


Figure 5. **(A)** Top-view illustration of our virtual setup for rendering the stimuli. The light pink and yellow rectangles represent the light source. **(B)** To make sure our experiment is asymmetric, we used different relief letter and a slightly different lighting to illuminate target and match images. Examples of target and match relief images used in [Experiment 1](#) for relief height = 0.5 mm and blur level of 0.2 mm.

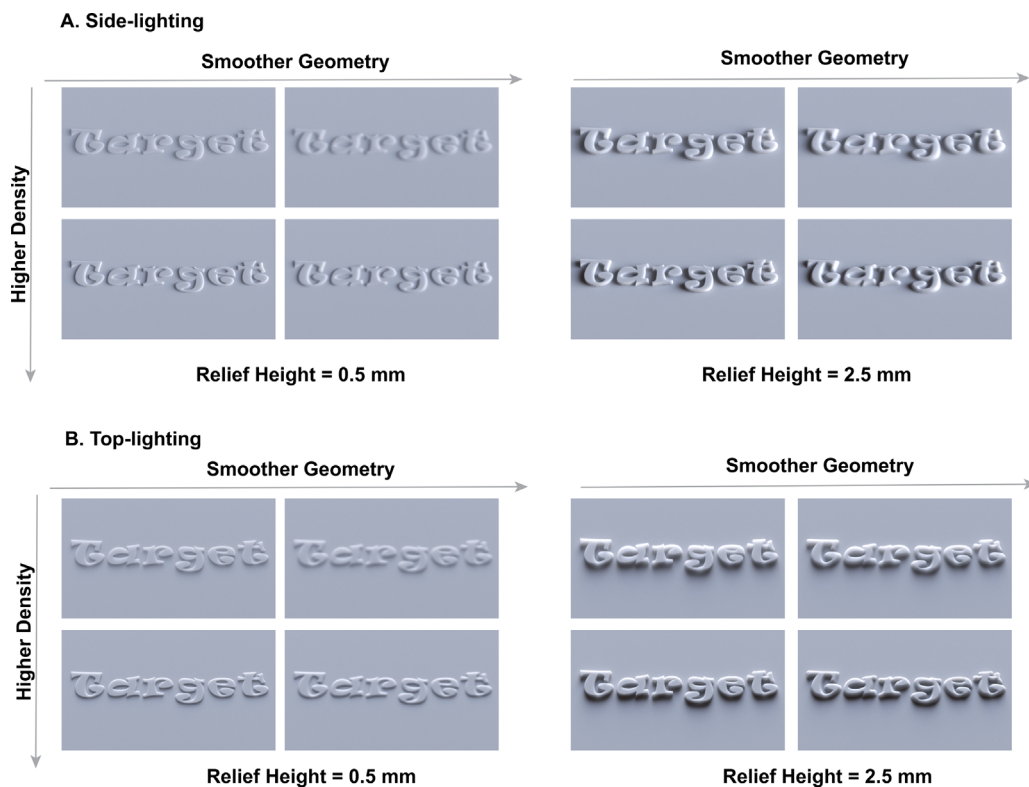


Figure 6. Experiment stimuli. We manipulate the 3D shape of our stimuli by adjusting the extrusion height and geometric sharpness. For each shape, we render the object with varying optical densities and illumination conditions. **(A)** Stimuli under a side-lighting condition. Within each panel, from left to right, we applied increasing Gaussian blur to the height fields and from top to bottom, the object has increasing optical density. Left panels: relief height = 0.5 mm; Right panels: relief height = 1.5 mm. **(B)** The same as **(A)** but under top lighting condition. Here, we only show target images as examples.

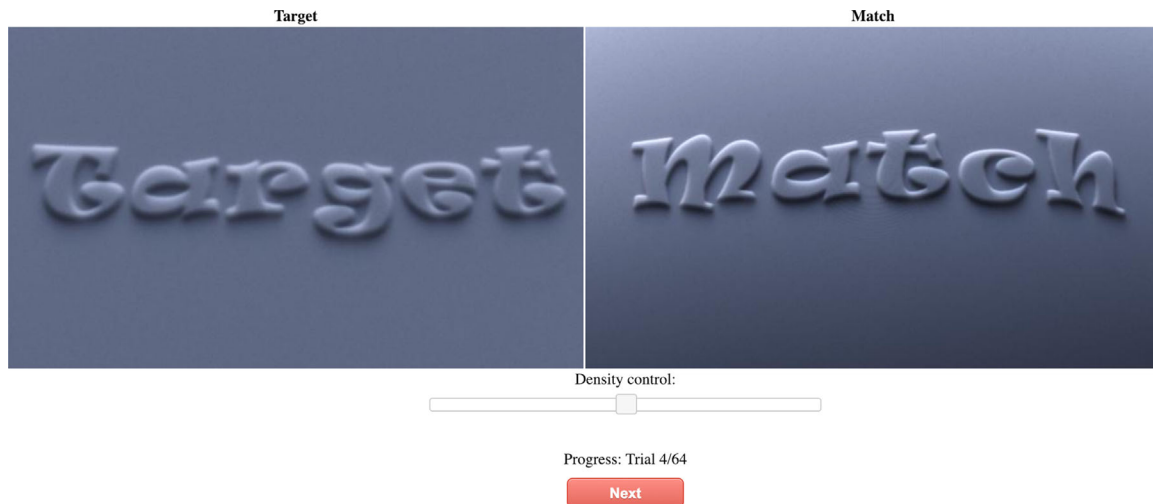


Figure 7. Experimental user interface of the translucency matching experiment. Human observers are asked to use the slider to adjust the optical density of the right (match) object, until its perceived material properties matches the appearance of the left (target) object. The match image always have a fixed blur level within each trial, which is different from that of the target image.

asymmetric matching was used to measure color constancy where subjects set asymmetric color matches between a standard object and a test object that were rendered under illuminants with different spectral power distributions. Besides color vision, asymmetric matching has also been used in material perception to understand the effect of surface gloss on color perception (Xiao & Brainard, 2008), the effect of illumination on perception of lightness and glossiness (Olkkonen & Brainard, 2010), the effect lighting direction on translucency (Xiao et al., 2014), the effect of distortion on transparency (Fleming et al., 2011), the effects of optical properties on perception of liquids (Assen & Fleming, 2016), and so on. It is an important method to measure how a particular factor affects material perception by preventing observers from performing low-level image matching.

To this end, we create a browser-based experiment interface to collect the matching data (see Figure 7). The experimental interface is coded using Javascript. The interface display two images. The object shown in the left (target) image has a fixed optical density. The interface provides a slider that allows observers to change the optical density of the object shown in the right (match) image.

Before the start of the experiment, observers are told that the images they would see were objects made of translucent materials, and they are shown some example stimuli images. As the experiment starts, observers are shown multiple pairs of images using the experiment interface. For each image pair, the specific instructions given to the observer are the following: “The reliefs in the images you will see in different trials are made with different materials. Your task is to match the perceived material properties of the soap in the right image to that in the left. To do so, you adjust the opacity of the object in the right image (match) to match the perceived

translucency to the object on the left (target). Notice that from trial to trial, the lighting direction can change (either side-lit or top-lit).”

Once they are satisfied with the match, the observers press the next button to confirm their response. After a response, the screen is blanked for 2 seconds, and subsequently a new image pair is shown. We call each such matching process a trial.

At each trial, the match object and target object are rendered with the same extrusion heights and the general similar lighting directions (both side or top but slightly different; see the Lighting section). The target object has a specific density value and a specific amount of blur, whereas the match object always has a fixed blur level (with kernel sd of 0.24 mm), which is never the same as the target. In total, the experiment consists of 160 trials, divided into 4 blocks of 40 trials each. There is no time limit for finishing each trial, and observers can take a break between the blocks.

In Experiment 2, we use the same procedure as described above for a different group of observers (see the section Observers).

Display

Observers performed the experiments in a dark room and the images were displayed on a 27-inch iMacPro monitor (Apple, Inc., Cupertino, CA; dynamic range: 60:1; color profile: sRGB; maximum luminance: 340 cd/m). The height of the image was 80 mm and the observers sat approximately 50 cm away from the monitor. The stimulus subtended 8.6° in visual angle.

Our rendered “RAW” images are float-valued and contain radiometric quantities (i.e., radiance values). To properly display the RAW images, we convert them into the sRGB color space using the standard

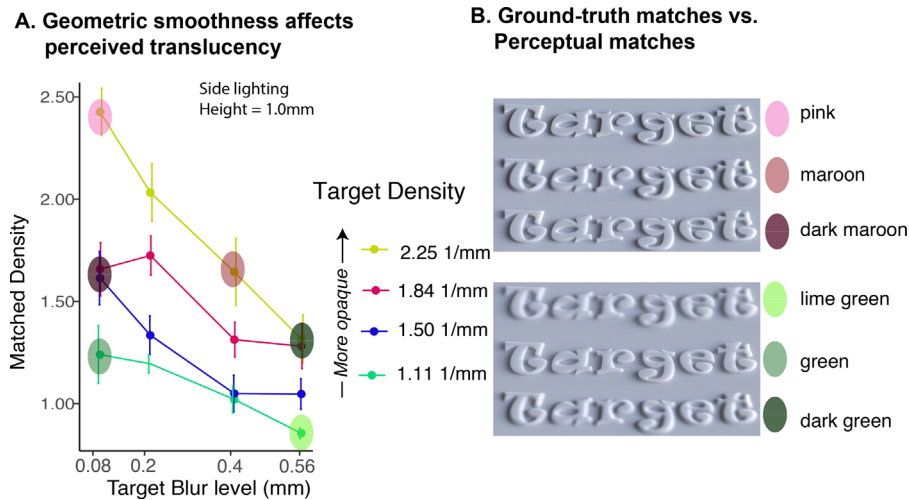


Figure 8. Asymmetric matching results and image demonstrations for [Experiment 1](#) with relief height 1.0 mm: blurring (smoothing geometric details) cause the object to appear more translucent (less opaque). **(A)** The mean match density across observers versus the level of blur. Different colors represent stimuli with different optical densities. **(B)** Demonstrations of perceptually equivalent image pairs versus pairs that have the same physical densities. Higher values indicates more opaque appearance. (Top) observers perceive an object with higher density and smooth geometry (middle image, maroon dot) to be equally translucent to an object with lower density and sharp geometry (lower image, dark maroon dot). The top image (pink dot) shows the physical ground-truth image of the object with the same density as the image shown in the middle row (maroon dot). (Bottom) observers perceive a target object with lower density (middle image, green dot) with sharp geometry to be equivalent to an object with higher density with smooth geometry (lower image, dark green dot). The top image shows the physical ground-truth image of the object with the same density as the target (lime green dot).

approach. This conversion is similar to applying $I_{sRGB} = I_{Raw}^{(1/2.2)}$, although they are not strictly identical. This conversion of color space (from linear RGB to sRGB) is the standard way to display rendered images (or measured RAW photos if that matters). Our monitors use the sRGB color gamut and are properly calibrated. This means that, when displaying a sRGB image, light physically emitted by our monitors will closely resemble the radiometric quantities recorded by the original simulated results.

Experiment 1: Positive relief

In [Experiment 1](#), we measure the effects of geometric sharpness on perceived translucency with the aforementioned asymmetric matching procedure using positive relief objects. Throughout the conditions, we also vary the optical density, relief heights, lighting conditions.

Observers

Thirteen observers (eight women; a mean age, 22.0 ± 2.5 years) participated in this experiment. All observers reported normal visual acuity and color vision. All

observers participated for credit in an introductory psychology course. The procedures were conducted in accordance with the Declaration of Helsinki and were approved by the Human Research Ethics Advisory Panel at American University.

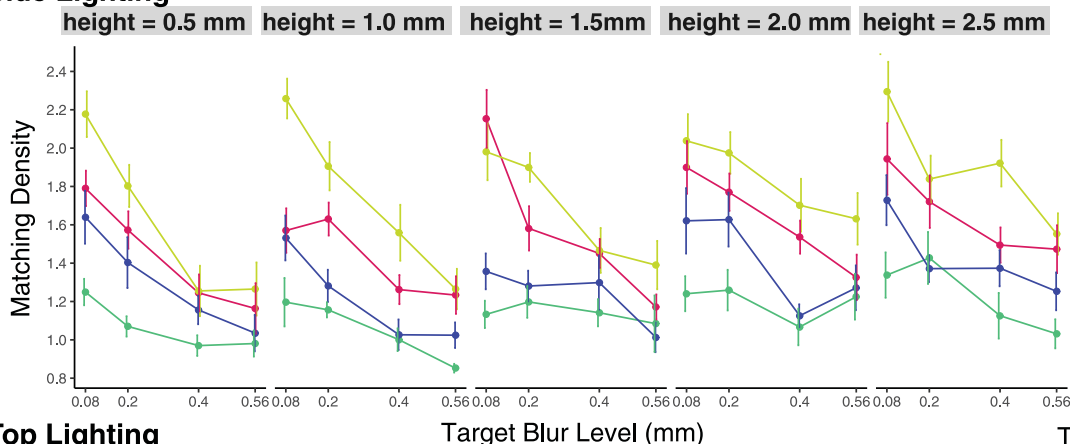
Results and discussion

[Figure 8A](#) demonstrates the mean match density across 13 observers versus blur levels for condition (height = 1.0 mm and lighting = “side-lit”), which is the same as the second panel on the top row in [Figure 9](#). We make the following observations.

We first note that observers can distinguish different optical densities when the target and the match have the same height and blur values. For these conditions, as the material optical density of the target increases, the matched density increases as well (e.g., the yellow line is well above the green line in [Figure 8A](#)). This shows that observers perceive objects with higher optical density to be more opaque.

On the other hand, as shown in [Figure 8A](#), when the blur level increases, the observers’ matched density decreases for each fixed target density. Put another way, to match the translucent appearance of the target object with the higher blur level, observers need to decrease the density of the match object. Equivalently,

A. Side Lighting



B. Top Lighting

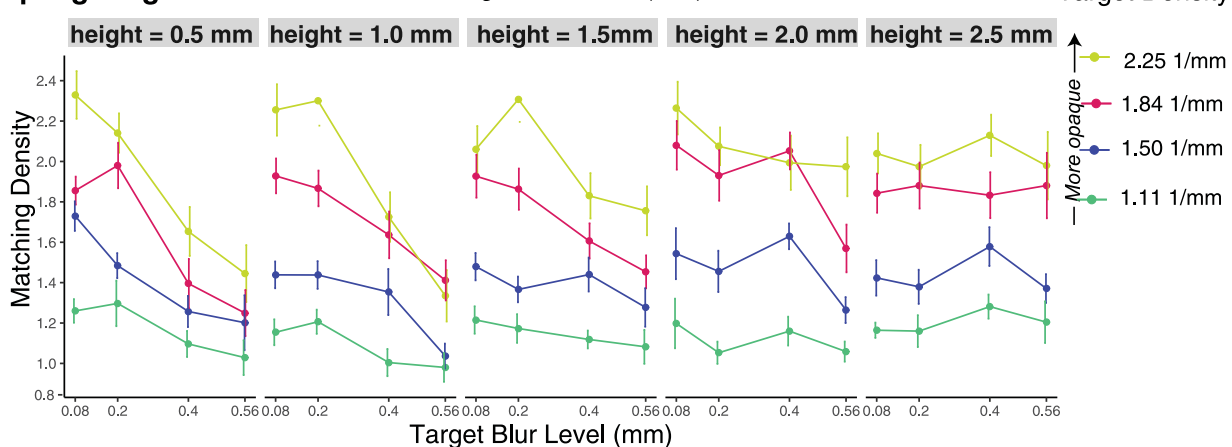


Figure 9. Results from [Experiment 1](#) (positive relief) for all relief heights and lightings. **(A)** Effect of geometric smoothness (applying Gaussian blur to 2D height fields) on the matching results for all relief heights under side lighting. Each panel plots the level of blur versus average match density for a specific relief height value. Higher values on the y-axis represents more opaque materials and lower values represent more translucent materials. From the left panel to the right, the relief heights increase. Different colors represents different optical densities for the target as shown in the figure legend. **(B)** Same plots as shown in **(A)** but for top-lighting conditions. For both lighting conditions, for the relief heights not at the highest level (i.e., left four panels), as blur level increases the mean match density decreases, suggesting observers perceive geometrically smoothed relief objects to be more translucent. At the highest relief level for top lighting (right most panel, bottom row) the effect is diminished (resulting in nearly flat lines).

this suggests that smoothing the height fields makes the object appear less dense optically (more translucent). To visually demonstrate this result, [Figure 8B](#) shows representative triplets of images, where the image of the target object is compared with the image of the perceptual match, as well as the image of the object that has the same ground-truth density as the target. The top panel of [Figure 8B](#) shows the effect of blur on translucent appearance of selected images. The middle image of the top panel is a cross-section of a blurred object which corresponds with the maroon dot on the data plot in [Figure 8A](#). The bottom image of the panel shows the image rendered with mean matched density across observers (dark maroon). Even though the perceptually matched object in this image has lower density and sharper features (lower blur level) than the target (red dot on data plot in [Figure 8A](#)),

observers perceive them to be similar in translucency. In contrast, the top image shows the object rendered with the same physical density as the target but with a lower blur level (pink dot on the data plot). Observers perceive this image to be more opaque than the target.

The bottom illustrates another example of the effect of blurring, where a translucent object with sharper features (middle, green dot) is perceived to be equivalent to a smoothed object (higher blur level) with higher density (bottom, dark green dot) in contrast with the object with the same physical density (top, lime dot). Together, this demonstrates that sharp geometries affect translucent appearance in such a way that a geometrically smoothed object appears more translucent than the sharp object that has the same optical density.

We further examine results for all other experimental conditions. **Figure 9** shows the average matching results for the relief objects for all five height conditions under both side (top) and top lighting (bottom) conditions. The format of **Figure 9** is the same as **Figure 8A**, where the x-axis represents the level of blurring applied to the height fields and the y-axis represents the matched density. From left to right, the plots show results for conditions with increasing heights of the relief. The top in **Figure 9** shows that geometric smoothness has a significant effect on perceived translucency, meaning that the mean matched density decreases as the blur increases. The prominence of this effect depends on the optical density. Blurring has a stronger effect for the high-density conditions (yellow, blue, and red lines) than for low-density (green lines). The same trend is observed for the top lighting conditions (**Figure 9**, bottom). Blur has a strong effect on low relief heights (left two plots) and the effect of blur on matched density is flattened for the higher relief values (right-most panel).

We perform a three-way within-subject analysis of variance on the difference between matched density and the target density with blur level, relief extrusion height and the lighting direction as independent variables. To summarize, we find a significant effect of blur on perceived translucency considering all the conditions such that, as blur increases, observers perceive the target objects to be more translucent. We also find significant main effects of relief heights and lighting on perceived translucency.

The results are as follows.

- *Blur level* has a significant main effect, $F(3, 2000) = 67.985, p < 0.001$,¹ such that as the amount of blurring increases, the value of $d_{\text{match}} - d_{\text{density}}$ decreases. The value is negative and its magnitude $\|d_{\text{match}} - d_{\text{density}}\|$ becomes larger, indicating that blur has a stronger effect for targets with higher densities.
- *Relief height* has a significant main effect, $F(4, 2000) = 5.497, p < 0.001$, such that larger values of relief height make the objects be perceived as less translucent (higher values of $d_{\text{match}} - d_{\text{density}}$). There is no significant interaction between blur level and relief height, $F(12, 2000) = 1.701, p = 0.0605$.
- *Lighting direction* also has a significant main effect, $F(1, 2000) = 22.788, p < 0.001$. There is no significant interaction between lighting and blur level, $F(3, 2000) = 1.122, p = 0.095$.

Experiment 2: Negative relief

The relief of objects in the real world (e.g., bas-relief sculptures or soaps) can be extruded positively or

negatively. To discover whether the effect of 3D shape on perceived translucency we observed in **Experiment 1** can be generalized to other shapes, we render a set of similar stimuli with negatively extruded geometries and measure the effects of geometric sharpness on perceived translucency.

Observers

Another 11 observers (eight women; mean age, 25.0 ± 3.5 years) participated in the experiment where we used negatively extruded objects (**Experiment 2**). All the other aspects of the procedure and methods are the same as **Experiment 1**.

Results and discussion

Figure 10 shows example stimuli with negative relief under two lighting conditions (side lighting, top lighting) and two relief heights (height = 0.5, 1.5 mm). Within each panel, the stimuli have increasing optical densities from the top to bottom rows ($d_{\text{target}} = 1.11, 2.25(1/\text{mm})$) and the blur level is increased from left to right (blur = 0.08, 0.56 mm). All the other rendering parameters are identical to the stimuli used in **Experiment 1**.

Figure 11 shows an example of the matching results for **Experiment 2** with negative relief (height = 0.5 mm, lighting = top), which is the same figure in second column of the lower row in **Figure 12**. Similar to **Figure 8**, **Figure 11** plots the matched densities against different levels of blur for each relief height level under top lighting. We show image examples of how blur affects perceived translucency, where the image of the target object is compared with the image of the perceptual match, as well as the image of the object that has the same ground-truth density as the target.

The top of **Figure 11B** shows the effect of blur on translucent appearance of the selected images. The middle image of the top is a cross-section of a blurred object which corresponds to the maroon dot on the data plot in **Figure 11A**. The bottom image shows the image rendered with mean matched density across observers (dark maroon dot). Even though the perceptually matched object in this image has lower density and sharper features (lower blur level) than the target (red dot on the data plot in **Figure 11A**), observers perceive them to be similar. In contrast, the top image shows the object rendered with the same physical density as the target but with a lower blur level (pink dot on the data plot). Observers perceive this image to be more opaque than the target. This experiment illustrates that geometrically blurring the object results in the observer perceiving the object to be more translucent.

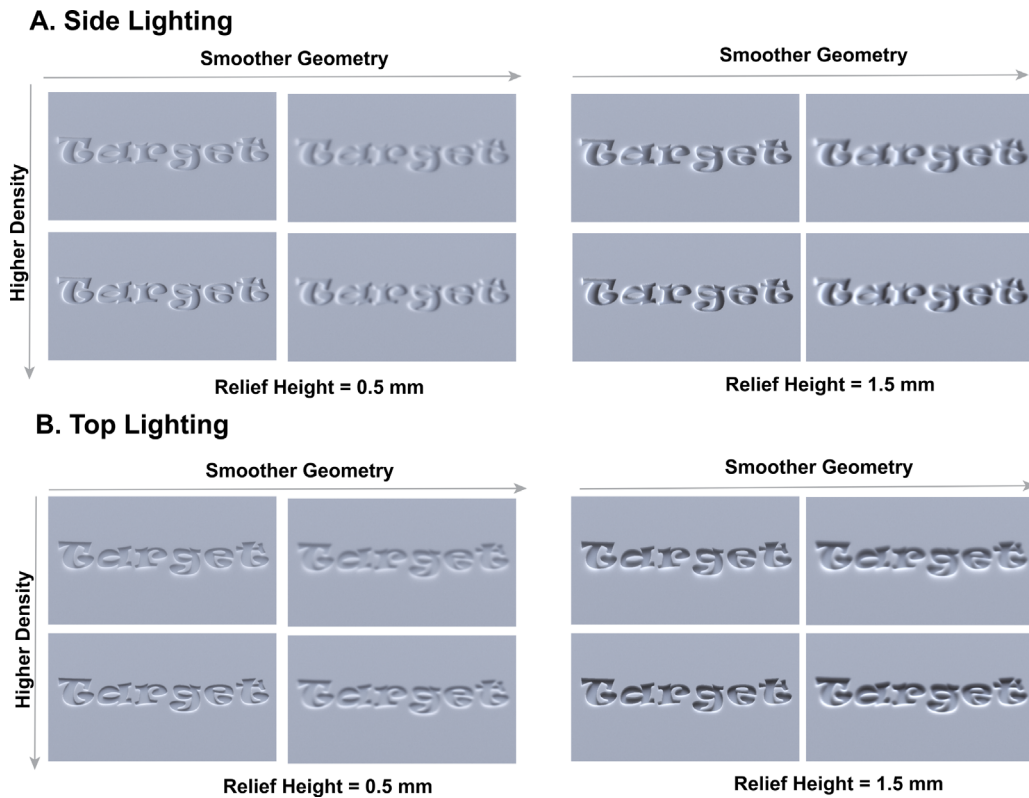


Figure 10. The conditions used in Experiment 2 are the same as in Experiment 1, except that the shape of the objects is different (negative relief). (A) Stimuli under side-lighting condition. Within each panel, from left to right, we applied increasing Gaussian blur to the height fields and from top to bottom, the object has increasing optical density. (Left): relief height = 0.5 mm. (Right): relief height = 1.5 mm. (B) The same as (A), but under top lighting.

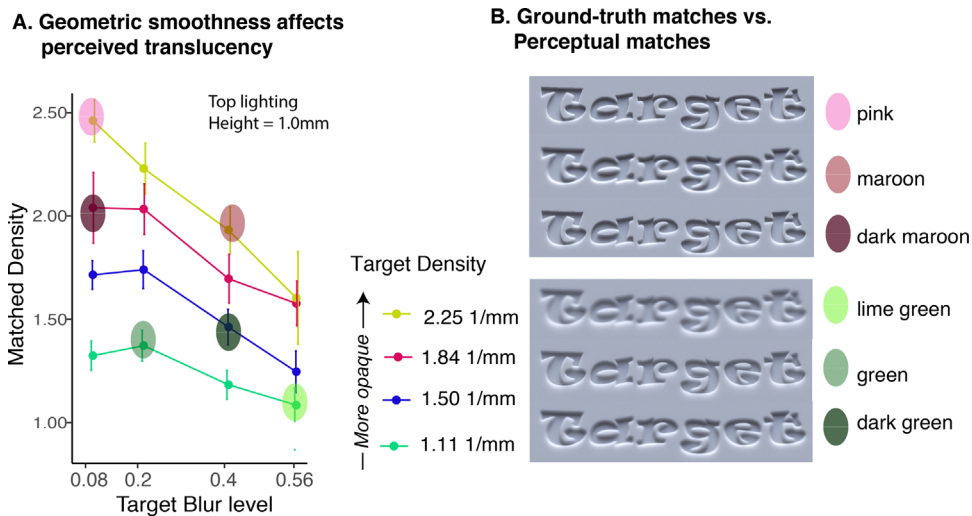


Figure 11. Results from Experiment 2 (negative relief) for all relief heights (depths) and lightings. (A) Mean match density versus levels of blur. (B) Demos of perceptually equivalent image pairs versus pairs that have the same physical densities. (Top) On average, observers perceive a target object with higher density (middle, maroon dot) with smooth geometry to be equivalent to an object with lower density but sharp geometry (bottom, darker maroon dot). The top image shows the physical ground-truth of the image of the object with the same density as the target, but with a lower blur level (pink). (Bottom) On average, observers perceive a target object with lower density (middle, green dot) with sharp geometry to be equivalent to an object with higher density but smooth geometry (bottom, dark green dot). The top image shows the physical ground-truth of the image of the object with the same density as the target (lime dot).

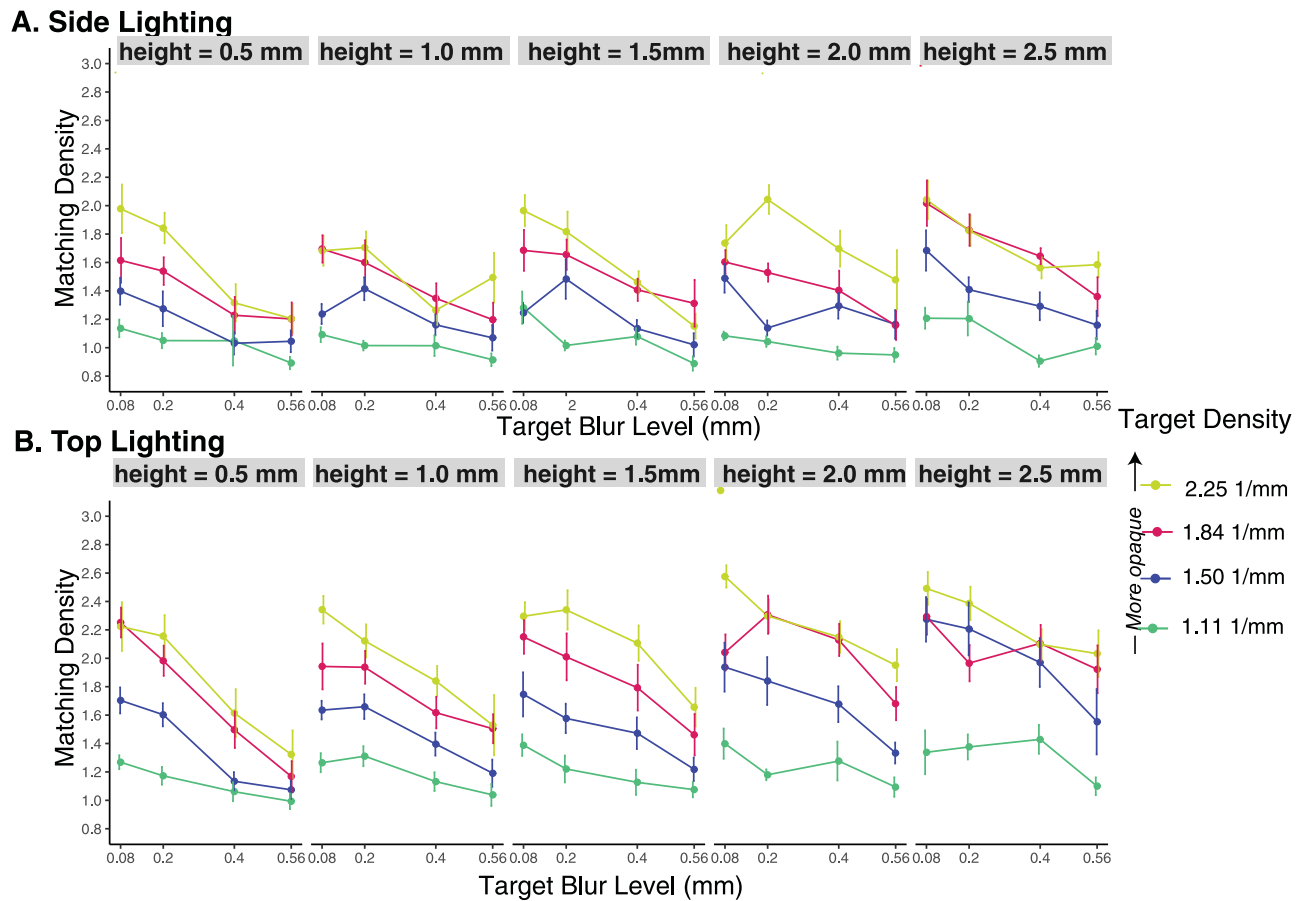


Figure 12. Results from the negative relief experiments. The effect of blurring on the match results for all relief heights and two lighting directions. **(A)** Data from the side lighting conditions. **(B)** Data from the top lighting conditions. Similar to the results from [Experiment 1](#), as geometric blur increased for the target, observers's matched density decreased, suggesting blur affect perceived translucency. Different colors represent different ground-truth densities for the target object.

Similar to [Experiment 1](#), the bottom triplets of images [Figure 11](#) demonstrated how an object with sharp features (middle row, green dot) could be perceived to be more opaque, which is equivalent to the stimuli with higher density (bottom, dark green dot) than a blurred object that has the same ground-truth density (top, lime dot).

[Figure 12](#) shows the mean matched density across observers for negative relief for all of the conditions. From left to right, the panels show data plots for stimuli with increased relief heights (i.e., deeper relief depths). The two rows show data from the two lighting conditions.

As in [Experiment 1](#), we find that blur has a significant effect on matched density on nearly all height conditions and both lighting conditions. In particular, observers perceive the blurred object to be more translucent than the unblurred object with the same density. Additionally, and again similar to [Experiment 1](#), blur has a stronger effect for the high density conditions (yellow and red lines) than the low density conditions (dark blue and green lines).

Similar to [Experiment 1](#), we perform a three-way within-subjects analysis of variance on the difference between matched density and the target density with blur level, relief height, and lighting direction as independent variables. The results are as follows:

- Similar to [Experiment 1](#), *blur level* has a significant main effect, $F(3, 1520) = 28.883$, $p < 0.001$, such that, as the amount of blur increases, the value of $d_{\text{match}} - d_{\text{target}}$ decreases.
- Also similar to [Experiment 1](#), *relief height* also has a significant main effect, $F(4, 1520) = 7.149$, $p < 0.001$, such that higher relief heights make the object appear less translucent (i.e., higher values of $d_{\text{match}} - d_{\text{target}}$). There is no significant interaction between blur level and relief height, $F(12, 1520) = 0.926$, $p = 0.5199$.
- Again similar to [Experiment 1](#), *lighting direction* does not have a significant main effect, $F(1, 1520) = 45.103$, $p < 0.001$. There is no significant interaction between lighting and blur level, $F(3, 1520) = 0.457$, $p = 0.7125$.

Discussion

Our results indicate that the perception of translucency depends not only on an object's optical parameters (e.g., scattering parameters used in rendering), but also on their 3D shapes. We use an asymmetric task where observers adjusted optical density of a match object to match the material properties of a target. In [Experiment 1](#) (with positive relief), we find that observers tend to perceive geometrically smoothed objects as more translucent than those with sharper geometries. This effect is significant across most relief heights and under both side and top lighting conditions except the highest relief under top lighting. In [Experiment 2](#) (with negative relief), we find similar effects of 3D geometry on translucency across all conditions. In the following, we discuss whether image contrast can be used to predict the same results.

What is the relationship between image contrast, geometric sharpness, and perceived translucency?

Previous work found that the human visual system might use image contrast as an image variable to initiate percepts of transparency and to assign transmittance to transparent surfaces ([Singh & Anderson, 2002](#)). A further study with more realistic images shows reducing contrast of the background decreases the perceived transparency of the overlaying filter ([Robilotto & Zaidi, 2004](#)) and studies on volumetric translucency also reveal significant effects of image contrast ([Fleming & Bühlhoff, 2005](#); [Motoyoshi, 2010](#)). Specifically, root mean square (RMS) contrast in high spatial frequency components in diffuse object images are suggested to be important for perceptual translucency in ([Motoyoshi, 2010](#)). A more recent work suggests global contrast is not related to translucency perception ([Nagai et al., 2013](#)). Here, we examine the relationship between image contrast, geometric sharpness, and the perceived translucency using our stimuli. To compare with the perceptual results, we first compute the difference in Michelson contrast between the target and the candidate match images $((I_{\max} - I_{\min}) / (I_{\max} + I_{\min}))$ and use this metric to make predictions of densities in a similar way as that has been described above.

[Figure 13](#) plots the predicted density based on the difference in Michelson contrast between target and match images for all experimental conditions. First, image contrast could discriminate different optical densities as well as the perceptual data. Second, the effect of geometric smoothness resembles perceptual data for the shallow relief such that, as blur increases, the predicted density decreases (see left two columns

in [Figure 13](#). However, as the relief height increases, the effect of blur on predicted density is diminished if not reversed (see right two columns in [Figure 13](#) in bottom rows), whereas in the perceptual data, increasing geometric smoothness would cause the matched density to decrease across all reliefs (see [Figure 9](#) and [Figure 11](#)). Hence, for the high relief conditions, the predictions from image contrast is opposite the perception data, suggesting observers are not using only image contrasts to judge translucent appearance.

To further examine the interaction between image contrast and geometric smoothness, we also plotted both the Michelson and RMS contrasts of all target images in the supplementary materials ([Supplementary Figure 1S](#) and [Supplementary Figure 2S](#)). First, consistent with previous findings, both image contrast measurements correlate strongly with optical densities such that increasing density will result in increased contrast, suggesting that image contrast is an important cue for perceived translucency. However, the relationship between contrast and geometric sharpness is a bit more complicated. For images with low relief, increasing geometric smoothness (blur) tends to slightly lower contrast. In contrast, for images with higher relief and especially higher densities, geometric smoothness tends to increase image contrast.

The interaction between geometric sharpness (or smoothness) and image contrast can be seen from examples shown in [Figure 6](#) and [Figure 10](#). For lower-relief conditions (e.g., images in [Figure 6](#), left), increasing geometric smoothness does not change much of the apparent image contrast. In fact, smoothing geometry might result in slightly reduced contrast owing to the dispersing of pixels with extreme intensities around the edge. For higher relief ([Figure 6](#), bottom right), especially for higher densities, it is speculated that increasing geometric smoothness increases image contrast owing to the expansion of darker or brighter image regions around the edge. The smoothed edges of a high relief object will cast more shadows and becomes slightly more glossy and brighter than sharp edges (e.g., the leftmost letter “t” in [Figure 6](#) [right] becomes brighter than the images on the left). Hence, images with rounder edges tend to have higher contrast than images with sharper edges when the relief is sufficiently high (such as 2.0 mm and 2.5 mm conditions corresponding to contrast values shown in yellow and lines in fourth and fifth columns in [Supplementary Figures 1S](#) and [2S](#)). These effects of smoothness on contrast could be even stronger for the images with negative reliefs as well ([Figure 10](#)). Owing to this interaction between image contrast and relief heights, the predictions generated from image contrast cannot fully explain the effects we found in perception. Overall, this analysis suggests that even though image contrast could be useful for the appearance of translucency

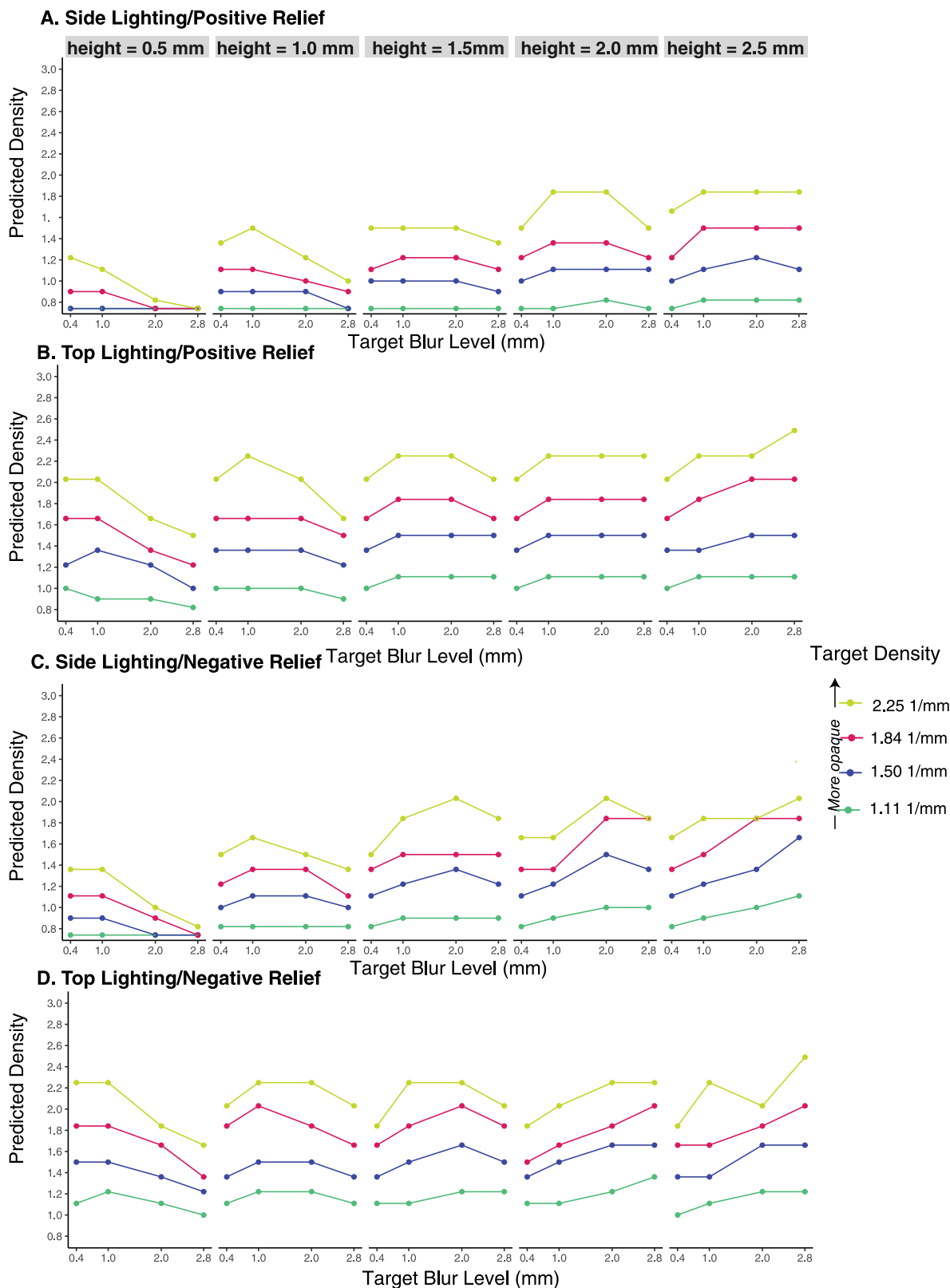


Figure 13. Prediction from image contrast: predicted matched densities by comparing Michelson Contrast (see main texts for details) between a target image and each of the candidate match images for all conditions in Experiments 1 and 2. (A) Predictions computed from images of positive relief under side lighting. From left to right, the images have increasing relief heights. (B) Predictions computed from images of positive relief under top lighting. (C) Same for negative relief under side lighting. (D) Same for negative relief under top lighting. The meaning of the symbols, legends, range of the X and Y axis are the same as those in Figure 9.

owing to changes in optical densities, it cannot explain the effects of geometric sharpness on translucency that we found in our perceptual data. Perhaps, future work should be investigated whether multiscale contrast could be a cue for translucency.

Conclusion

We performed psychophysical experiments, using physically based rendering to synthesize visual stimuli, and asked observers to match the perceived level of translucency of stimuli showing objects of different 3D geometric sharpness. We discovered that the perceived translucency depends not only on the material scattering parameters, but also on the objects' 3D geometries. Observers tend to perceive geometrically smooth objects to be more translucent than geometrically sharp objects, across different lighting direction and relief shape. Analysis of image contrasts of the images suggests that, even though image contrast could be a cue for estimating translucency for some shape conditions, it cannot fully predict our perceptual data. This finding suggests image contrast is not the only cue used by the visual system. Our results indicate that modifying the finely detailed 3D shapes of translucent objects could also alter their perceived appearance.

The findings reported in this article have implications in designing perception-aware metrics for translucency and 3D fabrication. Translucent objects with the same material properties but different fine 3D shape might appear different. In contrast, it is also possible to fabricate objects with the same overall perceived appearance, by using different physical materials and carefully manipulating the objects' fine 3D geometry. This suggests that, when fabricating objects with an objective to match a specific material appearance, their 3D shape must also be considered.

Keywords: material perception, translucency, 3D shape, volumetric scattering

Acknowledgments

Supported by NSF Grants CHS-1930755 and CHS-1900783 to KB from National Science Foundation and grants from American University to BX. We thank the American University High Performance Computing Facility (Zorro) for image renderings. We thank Pascal Barla and Shaiyan Keshvari for helpful comments on a draft version of the manuscript.

Commercial relationships: none.
Corresponding author: Bei Xiao.
Email: bxiao@american.edu.

Address: Department of Computer Science, American University, Washington, DC, USA.

Footnote

¹There are two parameters in a F test, for example, in F(3,2000), 3 means condition number, 2000 means sample number.

References

- Adams, W. J., & Elder, J. H. (2014). Effects of specular highlights on perceived surface convexity. *PLoS Computational Biology*, *10*(5), e1003576.
- Anderson, B. L. (2011). Visual perception of materials and surfaces. *Current Biology*, *21*(24), R978–R983.
- van Assen, J. J. R., & Fleming, R. W. (2016). Influence of optical material properties on the perception of liquids. *Journal of Vision*, *16*(15), 12–12.
- Barron, J. T., & Malik, J. (2015). Shape, illumination, and reflectance from shading. *IEEE Transactions on Pattern Analysis and Machine Intelligence*, *37*(8), 1670–1687.
- Brainard, D. H., & Wandell, B. A. (1992). Asymmetric color matching: How color appearance depends on the illuminant. *JOSA A*, *9*(9), 1433–1448.
- Chandrasekhar, S. (1960). *Radiative transfer*. North Chelmsford, MA: Courier Corporation.
- Chowdhury, N. S., Marlow, P. J., & Kim, J. (2017). Translucency and the perception of shape. *Journal of Vision*, *17*(3), 17–17.
- Debevec, P. (1998). Rendering synthetic objects into real scenes: Bridging traditional and image-based graphics with global illumination and high dynamic range photography. *Proceedings of the 25th annual conference on computer graphics and interactive techniques* (pp. 189–198).
- Doerschner, K., Yilmaz, O., Kucukoglu, G., & Fleming, R. W. (2013). Effects of surface reflectance and 3d shape on perceived rotation axis. *Journal of Vision*, *13*(11), 8–8.
- Donner, C., & Jensen, H. W. (2008). Rendering translucent materials using photon diffusion. *Acm siggraph 2008 classes* (p. 4).
- Fleming, R. W., & Bühlhoff, H. H. (2005). Low-level image cues in the perception of translucent materials. *ACM Transactions on Applied Perception (TAP)*, *2*(3), 346–382.
- Fleming, R. W., Jäkel, F., & Maloney, L. T. (2011). Visual perception of thick transparent materials. *Psychological Science*, *22*(6), 812–820.

- Fleming, R. W., Jensen, H. W., & Bülthoff, H. H. (2004). Perceiving translucent materials. *Proceedings of the 1st symposium on applied perception in graphics and visualization* (pp. 127–134).
- Gkioulekas, I., Walter, B., Adelson, E. H., Bala, K., & Zickler, T. (2015). On the appearance of translucent edges. *Proceedings of the IEEE conference on computer vision and pattern recognition* (pp. 5528–5536). IEEE.
- Gkioulekas, I., Xiao, B., Zhao, S., Adelson, E. H., Zickler, T., & Bala, K. (2013). Understanding the role of phase function in translucent appearance. *ACM Transactions on Graphics (TOG)*, 32(5), 147.
- Ho, Y.-X., Landy, M. S., & Maloney, L. T. (2008). Conjoint measurement of gloss and surface texture. *Psychological Science*, 19(2), 196–204.
- Inoshita, C., Mukaigawa, Y., Matsushita, Y., & Yagi, Y. (2012). Shape from single scattering for translucent objects. In *Computer Vision—eccv 2012* (pp. 371–384). New York: Springer.
- Ishimaru, A. (1991). Wave propagation and scattering in random media and rough surfaces. *Proceedings of the IEEE*, 79(10), 1359–1366.
- Jakob, W. (2010). Mitsuba renderer, 2010. <http://www.mitsuba-renderer.org>.
- Jensen, H. W., Marschner, S. R., Levoy, M., & Hanrahan, P. (2001). A practical model for subsurface light transport. *Proceedings of the 28th annual conference on computer graphics and interactive techniques* (pp. 511–518). New York, NY, United States: Association for Computing Machinery (ACM).
- Kim, J., Marlow, P. J., & Anderson, B. L. (2012). The dark side of gloss. *Nature Neuroscience*, 15(11), 1590.
- Kim, M., Wilcox, L. M., & Murray, R. F. (2016). Perceived three-dimensional shape toggles perceived glow. *Current Biology*, 26(9), R350–R351.
- Koenderink, J. J., & van Doorn, A. J. (2001). Shading in the case of translucent objects. In: *Human vision and electronic imaging vi* (Vol. 4299, pp. 312–320). SPIE, Bellingham, Washington USA: International Society for Optics and Photonics.
- Marlow, P. J., & Anderson, B. L. (2013). Generative constraints on image cues for perceived gloss. *Journal of Vision*, 13(14), 2–2.
- Marlow, P. J., & Anderson, B. L. (2015). Material properties derived from three-dimensional shape representations. *Vision Research*, 115, 199–208.
- Marlow, P. J., Kim, J., & Anderson, B. L. (2012). The perception and misperception of specular surface reflectance. *Current Biology*, 22(20), 1909–1913.
- Marlow, P. J., Kim, J., & Anderson, B. L. (2017). Perception and misperception of surface opacity. *Proceedings of the National Academy of Sciences*, 114(52), 13840–13845.
- Mooney, S. W., Marlow, P. J., & Anderson, B. L. (2019). The perception and misperception of optical defocus, shading, and shape. *eLife*, 8, e48214, doi:10.7554/eLife.48214.
- Moore, K. D., & Peers, P. (2013). An empirical study on the effects of translucency on photometric stereo. *Visual Computer*, 29(6-8), 817–824.
- Motoyoshi, I. (2010). Highlight-shading relationship as a cue for the perception of translucent and transparent materials. *Journal of Vision*, 10(9), 6–6.
- Nagai, T., Ono, Y., Tani, Y., Koida, K., Kitazaki, M., & Nakauchi, S. (2013). Image regions contributing to perceptual translucency: A psychophysical reverse-correlation study. *i-Perception*, 4(6), 407–428.
- Norman, J. F., Todd, J. T., & Orban, G. A. (2004). Perception of three-dimensional shape from specular highlights, deformations of shading, and other types of visual information. *Psychological Science*, 15(8), 565–570.
- Olkkonen, M., & Brainard, D. H. (2010). Perceived glossiness and lightness under real-world illumination. *Journal of Vision*, 10(9), 5–5.
- Olkkonen, M., & Brainard, D. H. (2011). Joint effects of illumination geometry and object shape in the perception of surface reflectance. *i-Perception*, 2(9), 1014–1034.
- Robilotto, R., & Zaidi, Q. (2004). Perceived transparency of neutral density filters across dissimilar backgrounds. *Journal of Vision*, 4(3), 5–5.
- Sawayama, M., Dobashi, Y., Okabe, M., Hosokawa, K., Koumura, T., Saarela, T., Olkkonen, M., . . . Nishida, S. (2019). Visual discrimination of optical material properties: a large-scale study. *BioRxiv*, 800870.
- Sawayama, M., & Nishida, S. (2018). Material and shape perception based on two types of intensity gradient information. *PLoS Computational Biology*, 14(4), e1006061.
- Singh, M., & Anderson, B. L. (2002). Toward a perceptual theory of transparency. *Psychological Review*, 109(3), 492.
- Todd, J. T., Egan, E. J., & Phillips, F. (2014). Is the perception of 3d shape from shading based on assumed reflectance and illumination? *i-Perception*, 5(6), 497–514.
- Todd, J. T., & Mingolla, E. (1983). Perception of surface curvature and direction of illumination

- from patterns of shading. *Journal of Experimental Psychology: Human Perception and Performance*, 9(4), 583.
- Vangorp, P., Laurijssen, J., & Dutr e, P. (2007). The influence of shape on the perception of material reflectance. *ACM transactions on graphics (tog)* (Vol. 26, p. 77). ACM.
- Wijntjes, M. W., Doerschner, K., Kucukoglu, G., & Pont, S. C. (2012). Relative flattening between velvet and matte 3d shapes: Evidence for similar shape-from-shading computations. *Journal of Vision*, 12(1), 2–2.
- Wijntjes, M. W., & Pont, S. C. (2010). Illusory gloss on lambertian surfaces. *Journal of Vision*, 10(9), 13–13.
- Xiao, B., & Brainard, D. H. (2008). Surface gloss and color perception of 3d objects. *Visual Neuroscience*, 25(3), 371–385.
- Xiao, B., Walter, B., Gkioulekas, I., Zickler, T., Adelson, E., & Bala, K. (2014). Looking against the light: How perception of translucency depends on lighting direction. *Journal of Vision*, 14(3), 17–17.
- Zhao, S., Ramamoorthi, R., & Bala, K. (2014). High-order similarity relations in radiative transfer. *ACM Transactions on Graphics (TOG)*, 33(4), 1–12.